Development of No-Flow Underfill Materials for Lead-Free Solder Bumped Flip-Chip Applications

Z. Q. Zhang, S. H. Shi, and C. P. Wong, *Fellow, IEEE*

***Abstract*—No-flow underfill process in flip-chip assembly has become a promising technology toward a smaller, faster and more cost-efficient packaging technology. The current available no-flow underfill materials are mainly designed for eutectic tin-lead (Sn/Pb) solders. With the advance of lead-free interconnection due to the environmental concerns, a new no-flow underfill chemistry needs to be developed for lead-free solder bumped flip-chip applications. Many epoxy resin/hexahydro-4-methyl phthalic anhydride (HMPA)/metal acetylacetonate material systems have been screened in terms of their curing behavior. Some potential base formulations with curing peak temperatures higher than 200 °C (based on differential scanning calorimetry at a heating rate of 5 °C/min) are selected for further study. The proper fluxing agents are developed and the effects of fluxing agents on the curing behavior and cured material properties of the potential base formulations are studied using differential scanning calorimetry (DSC), thermomechanical analyzer (TMA), dynamic-mechanical analyzer (DMA), thermogravimetric analyzer (TGA), and rheometer. Fluxing capability of the developed no-flow formulations is evaluated using the wetting test of lead-free solder balls on a copper board. The developed no-flow underfill formulations show sufficient fluxing capability and good potential for lead-free solder bumped flip-chip applications.**

***Index Terms*—Epoxy resin, flip-chip, lead-free solder, microelectronic packaging, no-flow underfill material.**

I. Introduction

THE RAPID advances of integrated circuit (IC) fabrication technology and the accelerated growth of the market for faster, smaller, yet less expensive products continue to challenge IC packaging technology [1], [2]. As a result, flip-chip technology on an organic substrate has been invented, developed, and practiced for more than ten years [3], [4]. Underfill technology is one of the keys to the success of flip-chip technology [5]. The conventional underfill technology has relied on capillary flow and has been developed for some time [6]. However, the current widely-used conventional underfill technology needs separate flux dispensing, solder bump reflow, flux cleaning, underfill dispensing and flow, and off-line underfill curing procedures. As such, the conventional underfilling process is tedious, expensive, and not transparent to the surface mount technology (SMT) facilities. Recently, a more promising underfill technology called no-flow underfill technology has been invented and developed [7]. The key to the success of the no-flow underfill technology lies in the availability of successful no-flow underfill materials, which have been developed for several years. Many flip-chip assemblies have been built and successfully demonstrated using no-flow assembling process [8]–[11].

Current flip-chip technology strongly relies on lead-containing soldering interconnection technology. However, the health threat from lead poisoning has made it imperative to remove lead from the solders. Lead-free soldering for the electronic industry has followed the global trend toward a lead-free environment. Although the proposal of eliminating lead-containing interconnects in microelectronic applications was initiated in the U.S. in the early 1990's, it has advanced much more rapidly in Japan and Europe. This differentiation in lead-free progress has triggered great concerns of lead-containing solder users about maintaining business opportunity, therefore further expediting the advancement of lead-free soldering programs. Along with this trend, it has been predicted that the current widely used lead-containing soldering interconnection technology in flip-chip applications will be gradually replaced by lead-free soldering technology such as tin-silver-copper (Sn/Ag/Cu) alloys in the near future.

Since the no-flow underfilling process reflows the solder joint and cures the underfill material concurrently, the curing temperature of a no-flow underfill material must be compatible with the melting point of the flip-chip bumping material. Sn/Ag/Cu system is more tolerant toward lead contamination and more compatible with the existing infrastructure for the transition stage than bismuth (Bi) containing systems, thus, it is one of the most potential materials being used in the future flip-chip bumping and is selected for study here. Formerly developed and currently available no-flow underfill materials are specifically designed for eutectic Sn/Pb solder bumping material, the melting point of which is 183 °C. They are not applicable to the Sn/Ag/Cu alloy bumped flip-chip assembling process since the melting point of Sn/Ag/Cu alloy is ∼217 °C. These no-flow underfill materials start to gel before the reflow of Sn/Ag/Cu bumps. In addition, current fluxes designed for eutectic Sn/Pb alloy might not have enough fluxing capability when applied to the Sn/Ag/Cu alloy system. Therefore, a new no-flow underfill chemistry needs to be developed for Sn/Ag/Cu bumping material.

Manuscript received April 25, 2000; revised October 30, 2000. This paper was recommended for publication by Associate Editor C. C. Lee upon evaluation of the reviewers' comments.

The authors are with the School of Materials Science and Engineering, Packaging Research Center, Georgia Institute of Technology, Atlanta, GA 30332-0245 USA (e-mail: cp.wong@mse.gatech.edu).

Publisher Item Identifier S 1521-3331(01)01947-X.

TABLE I
BASIC CURING PROPERTIES OF ERL 4221/HMPA/METAL ACETYLACETONATE FORMULATIONS

Metal Chelate	Melting point (°C)	Solubility in ERL 4221	Onset Temperature (°C)	Peak Temperature (°C)	Curing property	
					30 min. @ 170°C	30 min. @ 170°C + 30 min. 230°C
Li(I) Acac.*	250°C	150°C	168°C	219°C, 322°C	cured	-
Na(I) Acac.	210°C	150°C	152°C	176°C	air bubble, brittle	cured
Be(II) Acac.	108°C	60-70°C	162°C	198°C, 259°C	not cured	cured
Mg(II) Acac.	259°C	not dissolved	-	315°C	not cured	brittle, crack
Ca(II) Acac.	175°C	150°C	112°C	257°C	not cured	brittle, crack
Sr(II) Acac.	220°C	150°C	101°C	227°C	not cured	brittle, crack
Ba(II) Acac.	320°C	150°C	165°C	282°C	not cured	cured
Ga(III) Acac.	194°C	150°C	100°C	181°C	cured	cured
In(III) Acac.	186°C	not dissolved	76°C	132°C	soft material	brittle, crack
Tl(III) Acac.	160-165°C	not dissolved	75°C	135°C	cured	cured
Pb(II) Acac.	159°C	not dissolved	83°C	179°C	cured	cured
Cu (II) BenzoylAc.**	not done	60-70°C	199°C	231°C	cured	cured
Cd(II) Acac.	235°C	not dissolved	95°C	200°C	cured, brittle	cured
Sc(III) Acac.	187-190°C	90°C	121°C	160°C	cured, brittle	cured
Y(III) Aacac.	102°C	90°C	97°C	158°C	cured, brittle	cured
Cu(II) Acac.	179°C	90°C	199°C	232°C	cured	cured
Ti(IV) Acac.	subl. 200°C	not dissolved	140°C	266°C	not cured	cured
Zr(IV) Acac.	-	cured	-	-	-	-
Hf(IV) Acac.	193°C	150°C	200°C	288°C	not cured	cured
Co (II) Acac.	166°C	60°C	156°C	207°C	not cured	cured
Co (III) Acac.	214°C	60°C	180°C	217°C	not cured	cured
Fe (II) Acac.	subl. 85°C	60°C	124°C	176°C	cured	cured
Fe (III) Acac.	175°C	60°C	50°C	149°C	cured	cured

II. EXPERIMENTS

A. Chemical Ingredients of No-Flow Underfill Material

Epoxy resin, epoxy-curing hardener, metal acetylacetonate catalyst, and fluxing agent were the four categories of chemicals used in this study. The epoxy resins evaluated here included cycloaliphatic epoxy resin ERL 4221 from Union Carbide and bisphenol A epoxy resin EPON 8281 from Shell Chemicals. The epoxy equivalent weights (EEW) of the two epoxy resins were 134 g and 187 g, respectively. The epoxy curing hardener was hexahydro-4-methylphthalic anhydride (HMPA) was 168.2 g/mol and its purity was more than 97%. The metal acetylacetonates studied were included in Table I. Most of the metal acetylacetonates were purchased from Research Organic/Inorganic Chemical Corp. and stored in the lab for more than ten years. However, Co(II) acetylacetonate, Co(III) acetylacetonate, and Fe(III) acetylacetonate were newly purchased from Aldrich Chemicals, Inc. The fluxing agent studied in this work was neither acidic nor basic. All the chemicals were used as received. The mixing ratio of all the four components depended on the epoxy types. The mixing weight ratio of ERL 4 221 : HMPA : metal acetylacetonate : fluxing agent was 100 : 106.5 : 0.83 : 5.2 or 100 : 106.5 : 0.83 : 8.3. The mixing weight ratio of EPON 8 281 : HMPA : metal acetylacetonate : fluxing agent was 100 : 76.4 : 0.71 : 4.4 or 100 : 76.4 : 0.71 : 7.06.

B. Preparation of Underfill Materials

The specified quantity of each metal acetylacetonate was added into the epoxy resin and stirred for ∼60 min at a temperature ranging from 60 °C to 100 °C, depending on the solubility of the metal acetylacetonate in each epoxy resin. Then a specified quantity of the hardener HMPA was added into the epoxy/metal acetylacetonate mixture and stirred for additional 30 min at room temperature. Finally, a specified quantity of the fluxing agent was added into the above mixture and stirred for additional 30 min at ∼60 °C. The materials were then stored in a freezer at −40 °C. Prior to any evaluation, all the formulations were warmed up to room temperature.

C. Measurement Methods

Lead-Free Solder Wetting on Copper Board: The copper foil laminated FR-4 board used for this study was first cleaned using the routine cleaning procedures: 5 min rinse/immersion in acetone, then 5 min in methanol, then in 50/50 HCl solution for

TABLE I (*Continued.*)
BASIC CURING PROPERTIES OF ERL 4221/HMPA/METAL ACETYLACETONATE FORMULATIONS

V(III) Acac.	184°C	90°C	148°C	193°C	cured	cured
Mo(III) Acac.	179°C	not dissolved	167°C	212°C	cured	cured
Mn(II) Acac.	172°C	150°C	166°C	205°C	cured	cured
Ru(III) Acac.	237°C	90°C	199°C	263°C	not cured	crack
Rh(III) Acac.	263°C	90°C	174°C	235°C	cured	cured
Pd(II) Acac.	132-205°C	not dissolved	94°C	205°C	cured, brittle	cured, brittle
Pt(II) Acac.	250°C	130°C	220°C	248°C	not cured	crack
Ni(II) Acac.	dec. 229°C	90°C	185°C	249°C	not cured	cured
La(III) Acac.	150°C	110°C	168°C	209°C	cured	cured
Pr(III) Acac.	139°C	not dissolved	98°C	209°C	cured, brittle	cured, brittle
Nd(III) Acac.	140°C	not dissolved	88°C	204°C	cured, brittle	cured, brittle
Sm(III) Acac.	138°C	not dissolved	94°C	203°C	cured, brittle	cured, brittle
Gd(III) Acac.	100°C	not dissolved	88°C	195°C	cured, brittle	cured, brittle
Tb(III) Acac.	101°C	not dissolved	92°C	206°C	cured, brittle	cured, brittle
Dy(III) Acac.	103°C	not dissolved	152°C	199°C	cured	cured
Ho(III) Acac.	104°C	110°C	148°C	189°C	cured	cured
Er(III) Acac.	103°C	not dissolved	97°C	187°C	cured, brittle	cured, brittle
U(II) Acac.	225°C	cured	-	-	-	-
Lu(III) Acac.	-	not dissolved	169°C	193°C	cured, brittle	cured
Tm(III) Acac.	97°C	not dissolved	165°C	202°C	not cured	cured
Th(II) Acac.	171°C	130°C	120°C	169°C	not cured	cured

Note: *: Acac. stands for acetylacetonate; **: BenzoylAc. stands for benzoylacetonate.

~20 s, followed by a thorough DI water rinse and clean air jet drying. The lead-free solder ball was prepared through the following procedure. A small block of Sn/Ag/Cu alloy was placed in mineral oil in a beaker. The mineral oil was heated to ~240 °C so that Sn/Ag/Cu alloy was melted. High-speed agitation was then applied. When many small metal drops were formed, the mineral oil was gradually cooled while maintaining the high-speed agitation. The small lead-free solder balls formed were then filtered out and thoroughly washed by isopropyl alcohol and acetone. In the wetting test, a lead-free solder ball was placed on a copper foil. Then, the no-flow underfill material was dispensed on the ball to cover the ball. The testing vehicle then went through the pre-profiled five-zone reflow oven. The spreading of the solder melt on the copper board was observed and recorded.

DSC Study on the Curing Behavior: To study the curing behavior of the underfill formulations, a modulated DSC instrument (by TA Instruments, Model 2920) was used. A sample of ~10 mg of a formulation at room temperature was placed into a hermetic DSC sample pan. For investigation of the curing profile, the sample was then heated in the DSC cell at 5 °C/min to 300 °C or 350 °C to obtain its curing heat flow diagram. The cured sample was left in the DSC cell and cooled to room temperature. The sample was reheated to 280 °C at 5 °C/min to obtain another heat flow diagram. The initial temperature of the heat flow step of the second diagram is defined as the DSC glass transition temperature (DSC Tg).

TMA Study on the Coefficient of Thermal Expansion (CTE): The CTE measurement of a cured material was performed on a TMA instrument (by TA Instruments, Model 2940). A specimen for TMA testing was prepared by heating a liquid formulation in an aluminum pan (37.5 mm diameter) to 250 °C in a convective oven at about 3 °C/min heating rate. The sample was continuously cured in the oven at 250 °C for additional 15 min. For some formulations, they were further heated to 290 °C and cured at this temperature for additional 30 min. After that, the sample was taken from the oven and cooled to room temperature. The aluminum pan was then peeled off. The two surfaces of the sample disc were polished to uniform thickness of 1–2 mm. A diamond saw was used to cut the polished sample into squares with dimensions of about 5×5

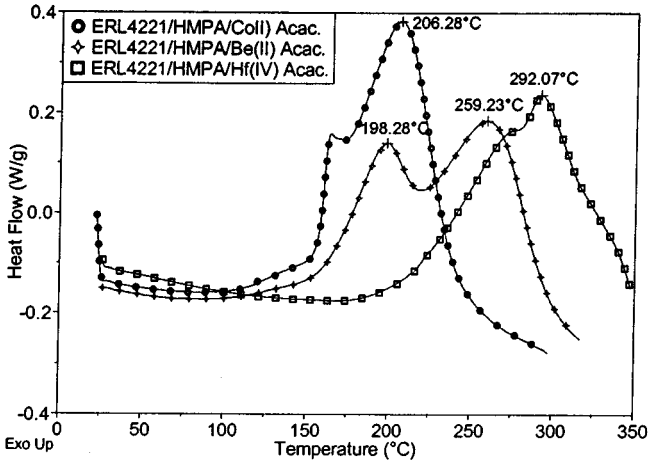

Fig. 1. DSC measured heat flow of three ERL4221/HMPA/metal Acac. formulations.

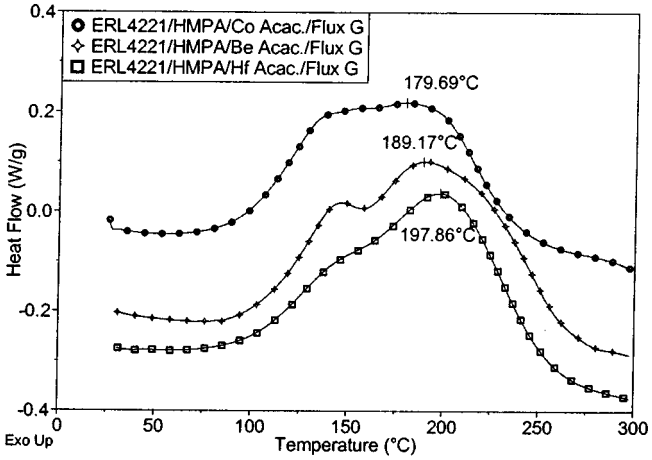

Fig. 2. DSC measured heat flow of the three formulations in Fig. 1 after addition of flux G.

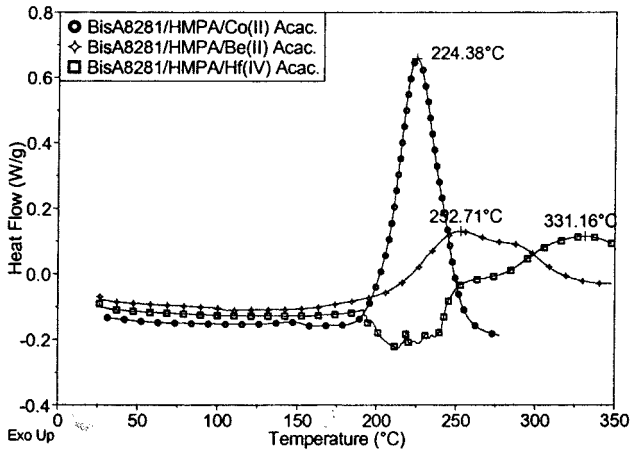

Fig. 3. DSC measured heat flow of three EPON8281/HMPA/metal Acac. formulations.

mm. The square sample was heated on the TMA sample stage to about 250 °C at a heating rate of 5 °C/min. The coefficient of thermal expansion (CTE) was obtained from the thermal expansion displacement versus temperature. The inflection point of thermal expansion was defined as TMA Tg. The CTE before TMA Tg was defined as α_1 and that after Tg as α_2.

DMA Study on Dynamic Moduli: Study on the dynamic moduli of a cured material was performed on a DMA instrument (by TA Instruments, Model 2980). The preparation of a specimen used for the DMA testing was the same as for the TMA testing. But the specimen size for DMA testing is longer and wider, about 32×11 mm. The measurement was performed under the single cantilever mode with 1 Hz sinusoidal strain loading. Storage modulus (E'), loss modulus (E"), and loss angle ($\tan\delta$) were calculated by the installed software.

TGA Study on Weight Loss and Thermal Stability: A TGA instrument (by TA Instruments, Model 2050) was used to investigate the weight loss of the formulations during curing. A sample of ~40 mg of a liquid formulation at room temperature was placed into a platinum TGA sample pan. The sample was then heated inside the TGA furnace at 10 °C/min to about 280 °C under N_2 purging (77 ml/min in vertical direction and 12 ml/min in horizontal direction). The weight difference between 25 °C and 270 °C was taken as the weight loss percentage of the formulation during curing. For thermal stability testing of a cured formulation, ~40 mg cured sample was put in the TGA sample pan and then heated from room temperature to 600 °C under the same N_2 purging condition. A curve of weight loss

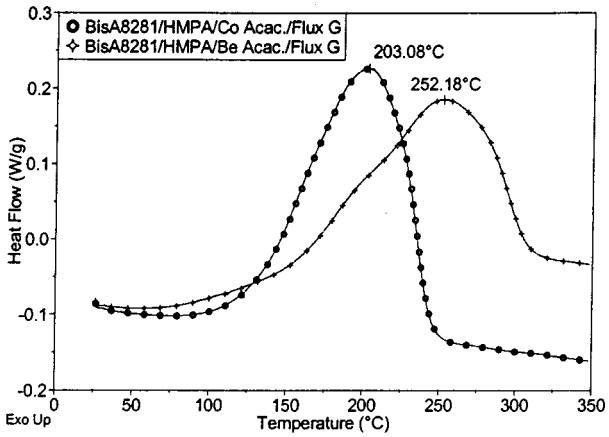

Fig. 4. DSC measured heat flow of the two formulations in Fig. 3 after addition of flux G.

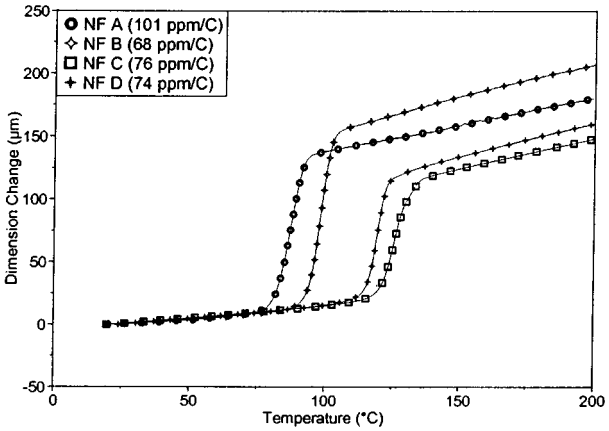

Fig. 5. TMA measured thermal expansion behavior of NF-A through NF-D (α_1 included).

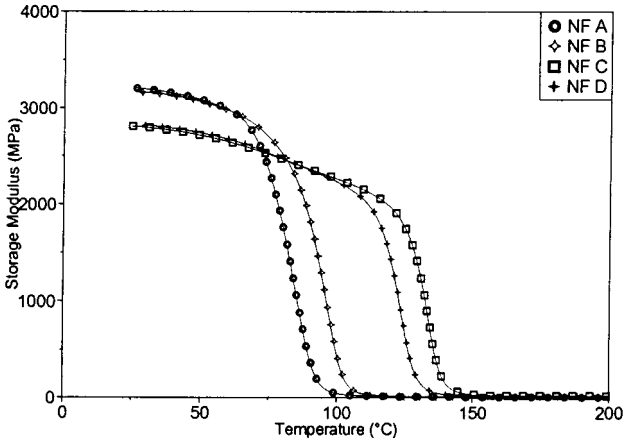

Fig. 6. DMA measured storage modulus change with temperature of NF-A through NF-D.

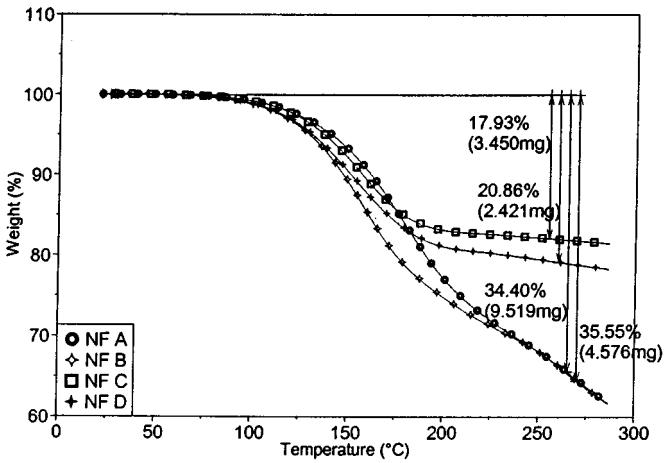

Fig. 7. TGA measured weight loss during heating of NF-A through NF-D.

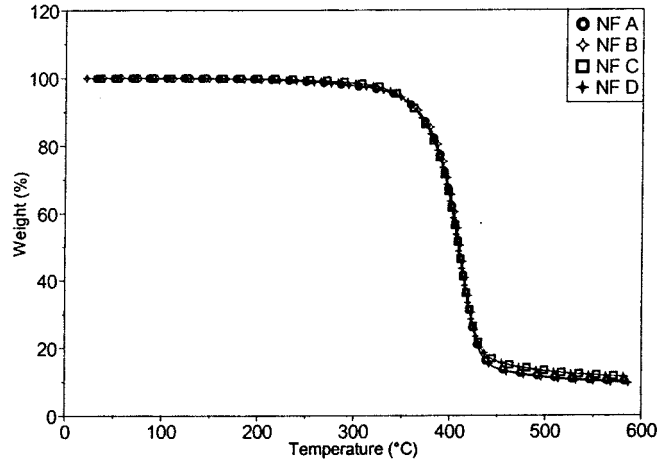

Fig. 8. TGA measured thermal stability of NF-A through NF-D.

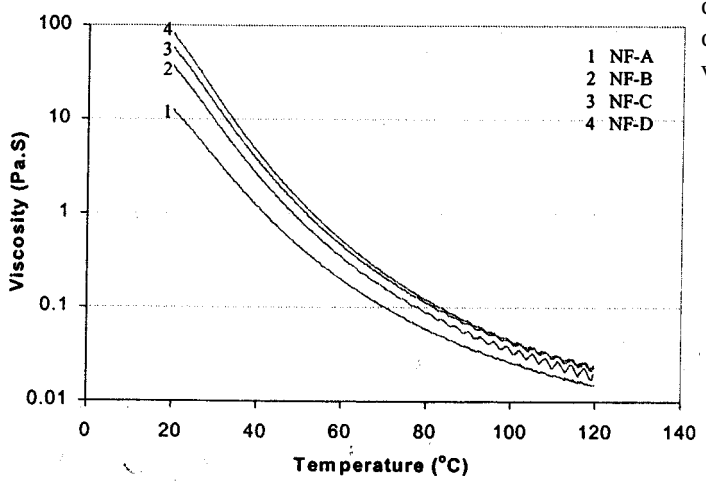

Fig. 9. Viscosity change with temperature for NF-A through NF-D.

versus temperature was then obtained. The onset temperature of the weight loss step was defined as the initial temperature of the decomposition of the cured sample.

Rheometer Study on the Viscosity and Pot-Life: A rheometer (by TA Instruments, Model AR1000-N) was used to measure the viscosity of the formulations. All the viscosity measurements

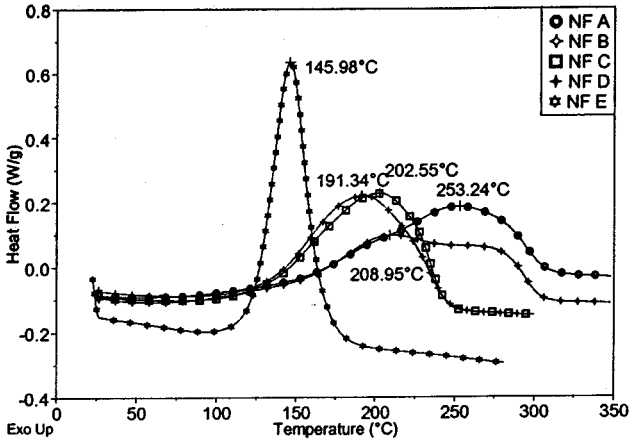

Fig. 10. DSC measured heat flow of NF-A through NF-E.

were performed under 10 S^{-1} constant shear strain rate mode with the temperature sweeping from 20 °C to 120 °C within 10 min. The viscosity change with temperature was recorded by the installed software.

III. Results and Discussion

A. Development of No-Flow Formulations for Lead-Free Solder

The development of no-flow formulations for lead-free solder bumped flip-chip applications started with the development of base formulations without the addition of the fluxing agent. Many ERL 4221/HMPA/metal acetylacetonate systems were screened in terms of the solubility of metal acetylacetonate in ERL 4221 epoxy resin and the curing properties of the prepared formulations, including curing onset temperature, curing peak temperature, and observed qualitative material properties after curing. The results are tabulated in Table I. There are four basic criteria in the selection of base formulations for next-stage development.

1) The metal ion does not have any potential to form mobile ions.
2) The metal acetylacetonate can be totally dissolved in ERL 4221 epoxy resin at a temperature lower than 150 °C. The existence of metal acetylacetonate particles may cause the variation of the cured material properties and adversely affect the interconnection yield due to the possible inclusion of the particles between solder bumps and bond pads.
3) The curing peak temperature must be higher than 200 °C based on DSC at a heating rate of 5 °C/min to ensure the required curing latency for lead-free solder reflow.
4) The material should be cured at 230 °C without any cracks after cooling. Higher curing temperature normally introduces higher residual stress and causes secondary reflow of the solder interconnects.

Based on these four criteria, only Be(II), Ba(II), Cu(II), Hf(IV), Co(II), Co(III), Rh(III), Ni(II), La(III) acetylacetonates qualify as the candidates. Among them, Co(II), Be(II), and Hf(IV) acetylacetonates are selected for further investigation toward the applicable no-flow underfill material in the next stage since these three catalysts can provide three typical curing peak

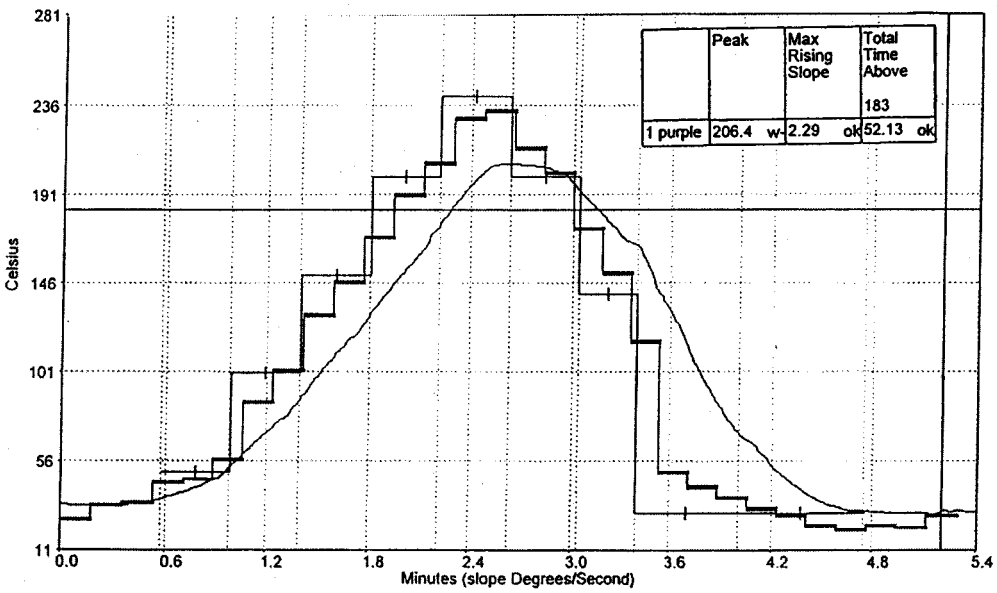

Fig. 11. Reflow profile for wetting test of lead-free solder balls.

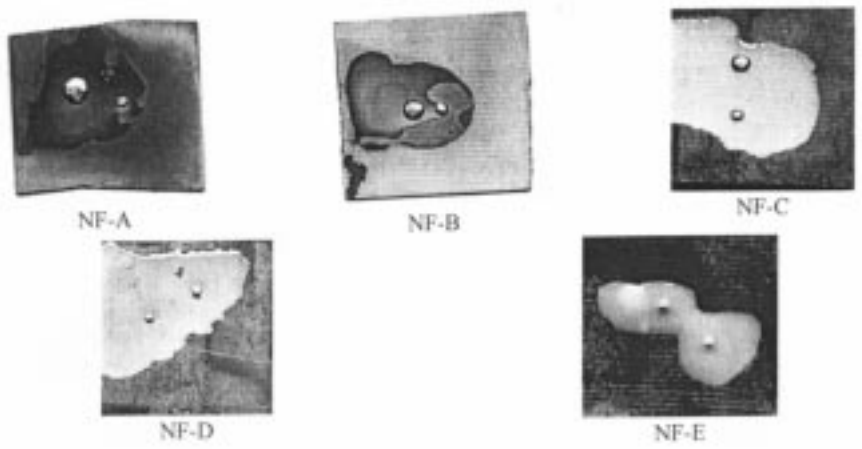

Fig. 12. Spreading of lead-free solder ball on copper board during reflow process.

temperatures for ERL 4221/HMPA systems. Their DSC curing heat flow diagrams are shown in Fig. 1.

In order to eliminate the metal oxide during reflow and facilitate the solder to wet on the copper surface, flux G was added to each formulation to provide the required fluxing capability for the three base formulations. The effects of the addition of flux G on the curing behavior are shown in Fig. 2. As can be observed in the figure, after the addition of flux G, the curing peak temperatures of the three base formulations are all below 200 °C. It indicates that the active hydrogen in flux G reacts with some of the anhydride in the system to form an acid, which has a higher reactivity than the anhydride for curing of the epoxy resin. The low curing peak temperatures may limit their applicability for lead-free solder bumped flip-chip applications. In order to formulate applicable no-flow materials with higher curing peak temperatures, metal acetylacetonate catalyzed EPON 8281/HMPA systems were investigated. The curing kinetics of three EPON 8281/HMPA systems catalyzed by Co(II), Be(II), and Hf(IV) acetylacetonates are shown in Fig. 3. Their curing peak temperatures are higher than those of the ERL 4221 based counterparts. However, the EPON 8281/HMPA/Hf(IV) Acac. formulation is not suitable for no-flow process for lead-free solder interconnecting due to its too high curing peak temperature. The effects of the addition of flux G on the curing kinetics of the other two formulations are shown in Fig. 4.

Although flux G still significantly reduces the curing peak temperatures, these formulations can maintain the curing peak temperatures higher than 200 °C. Therefore, the further material property characterization and fluxing capability evaluation were conducted on the Be(II) and Co(II) catalyzed EPON 8281 based formulations. The names of the developed four no-flow underfill materials are NF-A, NF-B, NF-C, and NF-D. The characterized material properties of the four underfill formulations are shown in Figs. 5–9. Fig. 5 shows the TMA measured thermal expansion behavior of the cured materials. The CTE's of the four materials before Tg (α_1) are listed in the legend of the figure. Fig. 6 shows the DMA measured storage modulus change with respect to the temperature. The weight loss of the four formulations during curing is shown in Fig. 7. It is observed that the weight losses are

high because the catalysts involved in these formulations have high latency and there is no significant reaction at the temperature when HMPA starts to evaporate. There are more significant weight losses in NF-A and NF-B whose curing peak temperatures are higher than those of NF-C and NF-D (see Fig. 10). This might become a potential concern in the application of no-flow underfill. Fig. 8 shows the thermal stability of cured samples. It can be concluded that the cured underfills have high thermal stability up to 350 °C, after which they start to degrade. Fig. 9 shows the viscosity change with temperature for the four formulations. Although the viscosity is high at room temperature, it decreases quickly with the increase in temperature. All the formulations have low enough viscosity beyond 100 °C for the chip to collapse and touch the bond pad in the process of no-flow underfill.

B. In-Situ Fluxing Capability Test

The DSC measured heat flow of five no-flow underfill materials NF-A through NF-E are shown in Fig. 10. NF-E is a commerically available no-flow underfill for eutectic Sn/Pb solder bumped chip application. The reflow porfile used for the wetting test is shown in Fig. 11. The spreading of the lead-free solder on the copper board after reflow are shown in Fig. 12. It is observed that NF-A, B, and C allowed lead-free solders to wet on the copper board while NF-D did not. It can be concluded that flux G can provide sufficient fluxing capability for lead-free solders. The wetting capability of the no-flow underfill is therefore determined by the curing behavior of the underfill. Comparing the results with the DSC measured heat flow curves in Fig. 10, it can be inferred that curing peak temperature higher than 200 °C may be required to ensure the wetting of the lead-free solder ball on copper board.

The *in-situ* fluxing capability test is a good indicator toward the application of developed no-flow underfill for the lead-free solder bumped flip-chip. Further assembly test using lead-free bumped chip and printed wiring board needs to be carried out to verify the success of the no-flow underfill. The potential concerns in the application includes the following.

1) The weight loss shown in Fig. 7 might cause voids in the package and has a negative effect on the reliability, in addition to the toxicity of anhydride released into the atmosphere.
2) The higher process temperature of lead-free solder requires a higher curing temperature of the underfill, compared to the case using the eutectic Sn/Pb solder, which will introduce higher residue stress when the whole package cools down to ambient temperature. Its influenced on the reliability needs to be addressed.
3) The fluxing capability of Flux G toward other surface finishes including Ni/Au, organic surface preservative (OSP), solder cap needs to be verified.

IV. CONCLUSIONS

Many ERL 4221/HMPA/metal acetylacetonate systems were screened for lead-free no-flow underfill applications. Several systems showed the potential for lead-free no-flow application. However, the addition of flux significantly reduced the curing peak temperatures and limited their applicability as a fluxing no-flow underfill material for lead-free solder. Several fluxing EPON 8281/HMPA/metal acetylacetonate systems were developed, which have higher curing peak temperatures and allow lead-free solder wetting on the copper board. For Sn/Ag/Cu alloy solder with the melting point at 217 °C, the developed no-flow underfill materials that have a curing peak temperature higher than 200 °C (based on DSC at a heating rate of 5 °C/m) are desired.

REFERENCES

[1] R. Marrs, "Trends in IC packaging," *Electron. Packag. Prod.*, pp. 24–30, Aug. 1996.
[2] R. R. Tummala, E. J. Rymaszewski, and A. Klopfenstein, *Microelectronics Packaging Handbook*, 2nd ed. New York: Chapman & Hall, 1997, pt. II.
[3] F. Nakano, T. Soga, and S. Amagi, "Resin-insertion effect on thermal cycle resistivity of flip-chip mounted LSI devices," in *Proc. Int. Society Hybrid Microelectron. Conf.'87*, 1987, p. 536.
[4] D. Suryanarayana, R. Hsiao, T. P. Gall, and J. M. McCreary, "Flip-chip solder bump fatigue life enhanced by polymer encapsulation," in *Proc. 40th IEEE Electron. Comp. Technol. Conf.'90*, 1990, p. 338.
[5] D. Suryanarayana and D. S. Farquhar, "Underfill encapsulant for flip chip applications," in *Chip on Board*, J. H. Lau, Ed. New York: Van Nostrand Reinhold, 1994, pp. 504–531.
[6] L. Nguyen *et al.*, "High performance underfills development- materials, process, and reliability," in *Proc. PEP'97*, 1997, p. 300.
[7] C. P. Wong, S. H. Shi, and G. Jefferson, "High performance no-flow underfills for low-cost flip-chip applications: material characterization," *IEEE Trans. Comp., Packag., Manufact. Technol. A*, vol. 21, p. 450, Sept. 1998.
[8] C. P. Wong, D. F. Baldwin, M. B. Vincent, B. Fennell, L. J. Wang, and S. H. Shi, "Characterization of a no-flow underfill encapsulant during the solder reflow process," in *Proc. 48th Electron. Comp. Technol. Conf.'98*, 1998, p. 1253.
[9] S. H. Shi and C. P. Wong, "Study of the fluxing agent effects on the properties of no-flow underfill materials for flip-chip applications," *IEEE Trans. Comp., Packag., Manufact. Technol. A*, vol. 22, p. 141, June 1999.
[10] C. P. Wong, S. H. Shi, and G. Jefferson, "High performance no-flow underfills for low-cost flip-chip applications: material characterization," *IEEE Trans. Comp., Packag., Manufact. Technol. A*, vol. 21, no. 3, pp. 450–458, 1998.
[11] N. C. Lee, "Lead-free soldering–where the world is going," *Adv. Microelectron.*, pp. 29–35, Sept./Oct. 1999.

Z. Q. Zhang received the B.S. degree from Fudan University, Shanghai, China, in 1997 and is currently pursuing the Ph.D. degree in the School of Materials Science and Engineering, Georgia Institute of Technology, Atlanta.

S. H. Shi received the B.S. degree from Tsinghua University, Beijing, China, in 1991, the M.S. degree from Fudan University, Shanghai, China, in 1994, and the Ph.D. degree in materials science and engineering from the Georgia Institute of Technology, Atlanta, in 2000.

He is now with Intel Corporation as a Senior Process Engineer

C. P. Wong (SM'87-F'92) received the B.S. degree in chemistry from Purdue University, West Lafayette, IN, and the Ph.D. degree in organic/inorganic chemistry from Pennsylvania State University, University Park.

After his doctoral study, he was awarded two years as a Postdoctoral Scholar at Stanford University, Stanford, CA. He joined AT&T Bell Laboratories, in 1977 as a Member of Technical Staff. he was elected an AT&T Bell Laboratories Fellow in 1992. He is a Regents Professor with the School of Materials Science and Engineering and a Research Director at the NSF-funded Packaging Research Center, Georgia Institute of Technology, Atlanta. His research interests lie in the fields of polymerica materials, high Tc ceramics, material reaction mechanism, IC packaging in particular, hermetic equivalent plastic packaging and electronic manufacturing packaging and reliability processes. He holds over 40 U.S. patents and numerous international patents, and has published over 270 technical papers and 290 presentations in the related area.

Dr. Wong was the IEEE Components, Packaging, and Manufacturing Technology (CPMT) Society President in 1992 and 1993. He is a member of the National Academy of Engineering.